Lattice Compression from Conduction Electrons in Heavily Doped Si:As

G. S. Cargill, III, J. Angilello, and K. L. Kavanagh[(a)]

IBM Research Division, Thomas J. Watson Research Center, Yorktown Heights, New York 10598

(Received 11 March 1988)

High-resolution x-ray scattering measurements on heavily doped Si:As (5×10^{21} As cm^{-3}) show lattice *compression* relative to pure silicon, $\Delta a/a = -0.0019\pm0.0003$, although extended x-ray-absorption fine-structure measurements show that the As−Si bond length is 0.06 ± 0.02 Å *greater* than the usual Si−Si bond length. The overall lattice compression is attributed to increased population of conduction-band states which reduces Si−Si bond lengths. These measurements provide the first direct measurement of the hydrostatic deformation potential for the conduction-band edge in silicon, $+3.3\pm0.7$ eV.

PACS numbers: 61.70.Sk, 61.70.At, 72.80.Cw

Effects of heterovalent, substitutional impurities on lattice parameters of elemental semiconductors are important in the determination of the degree of lattice mismatch in doped superlattices and in other heterostructures. Also, experimental determinations of impurity effects on local atomic arrangements and on lattice parameters are needed to test the accuracy of first-principles calculations.[1-3]

By combining measurements of lattice parameters by x-ray scattering with measurements of local interatomic distances by extended x-ray-absorption fine-structure (EXAFS) spectroscopy for As-doped Si (Si:As), we have found that As-to-Si bond lengths are 0.06 ± 0.02 Å *greater* than the usual Si−Si bond length,[4] yet the Si:As lattice parameter $a_{\mathrm{Si:As}}$ is reduced relative to the lattice parameter of pure Si, a_{Si}. We have determined the conduction-band-edge deformation potential for Si from these measurements.[5]

This is the first instance for dopants in Si or Ge in which both local displacements and overall lattice parameters have been measured. The results provide a new, critical test of theoretical predictions for the conduction-band-edge hydrostatic deformation potential and for effects of donors on lattice parameters in silicon.[1,2]

Si:As samples were prepared by ion implanting of (100) Si wafers, (Czochralski grown, B doped, 10–20 Ω cm) with As, 6×10^{16} cm^{-2} and 100 keV, followed by laser annealing with a frequency-doubled Nd-doped yttrium-aluminum-garnet Q-switched laser.[4,6] For these samples, most of the As is contained within a 1500-Å-thick near-surface layer as illustrated in Fig. 1(a), with a maximum concentration of $N_{\mathrm{As}}=5\times10^{21}$ cm^{-3} ($x_{\mathrm{As}}=0.10$). For samples prepared in this way, at least 90% of the As is substitutional and electrically active.[6-8] Some samples were also subsequently annealed for 30 min at temperatures between 200 and 600 °C. These treatments increased the electrical resistivity because of the progressive electrical deactivation of the arsenic but did not produce a significant change in the As concentration profile $x_{\mathrm{As}}(z)$.[6,8,9]

Lattice parameter measurements were made as shown in Fig. 1(b), with a channel-cut Ge(111) monochromator and Cu-$K\alpha_1$ radiation. EXAFS measurements, with

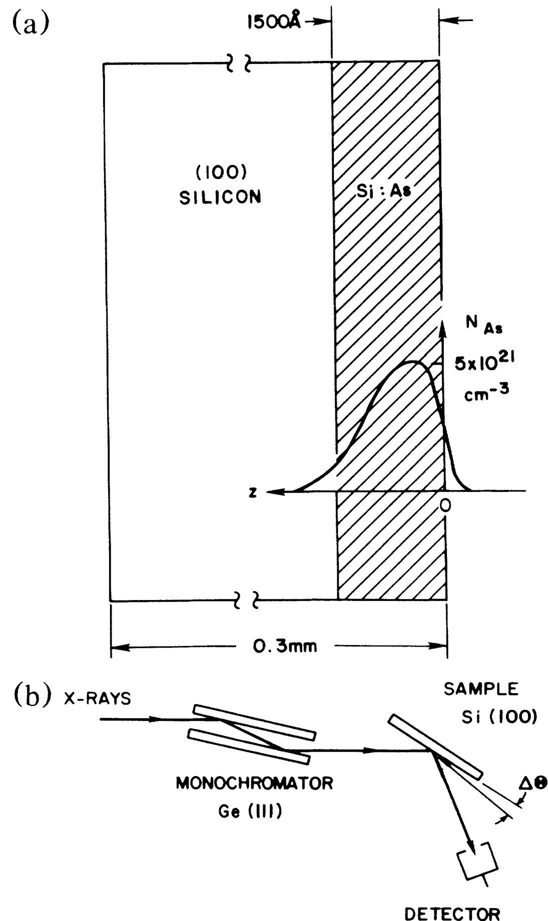

FIG. 1. (a) Cross-section view of ion-implanted, laser-annealed Si:As samples used for x-ray scattering and EXAFS measurements. Inset: Depth dependence of the As concentration. (b) Experimental configuration for high-resolution x-ray scattering measurements of lattice parameters (rocking curves) for Si:As samples.

© 1988 The American Physical Society

total electron yield detection,[10] were made at the Cornell High Energy Synchrotron Source.

X-ray rocking curves for an as-laser-annealed Si:As sample and for pure Si are shown in Fig. 2(a). The contribution from the As-containing near-surface layer is clearly visible as a satellite peak displaced to a larger scattering angle from pure Si by $\Delta\Theta = 300 \pm 50$ s. If the perpendicular strain within the near-surface layer were uniform, this observed displacement would indicate a fractional change in the (400) interplanar spacing of $\Delta d/d = -(2.1 \pm 0.3) \times 10^{-3}$. However, the perpendicular strain distribution $\Delta d(z)/d$ is expected to be proportional to the As concentration $N_{\mathrm{As}}(z)$, which is nonuniform [see Fig. 1(a)]. By using a Gaussian to represent $N_{\mathrm{As}}(z)$ and $\Delta d(z)/d$ in kinematic modeling of the x-ray rocking curve, the perpendicular strain for maximum As concentration was determined to be $(\Delta d/d)_{\max} = -(3.4 \pm 0.6) \times 10^{-3}$ for the as-laser-annealed Si:As sample.[11]

For situations like that shown in Fig. 1(a), where an overlayer is laterally constrained by its substrate, measurements of perpendicular strain for the overlayer should be corrected for Poisson expansion to obtain the lattice parameter $a_{\mathrm{Si:As}}$ which the overlayer would have if it were not constrained.[12] In the case of (100) Si, this is given by

$$\frac{a_{\mathrm{Si:As}} - a_{\mathrm{Si}}}{a_{\mathrm{Si}}} = \frac{\Delta a}{a} = \frac{\Delta d_{400}}{d_{400}} \frac{c_{11}}{c_{11} + 2c_{12}}, \tag{1}$$

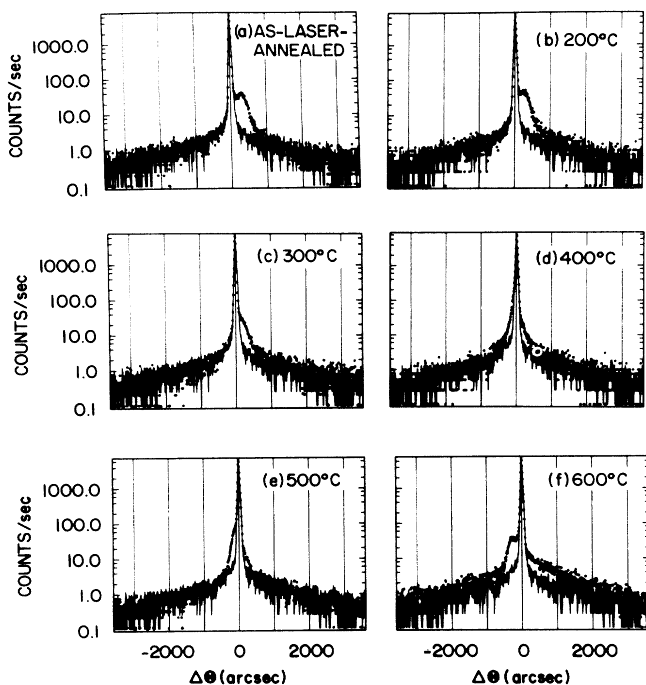

FIG. 2. X-ray rocking curves (400) for (a) an as-laser-annealed Si:As sample, and (b)-(f) pure Si samples after subsequent 30-min anneals at the indicated temperatures. In each case, the solid line is the rocking curve for pure silicon.

with elastic constants $c_{11}/(c_{11} + 2c_{12}) = 0.56$. For the as-laser-annealed Si:As sample, this yields

$$\Delta a/a = -(1.9 \pm 0.3) \times 10^{-3}$$

or

$$\beta_{\mathrm{total}} = \frac{\Delta a}{a N_{\mathrm{As}}} = -(0.4 \pm 0.1) \times 10^{-24}\ \mathrm{cm}^3, \tag{2}$$

with $N_{\mathrm{As}} = (5.0 \pm 0.5) \times 10^{21}\ \mathrm{cm}^{-3}$.

The correction for the Poisson expansion, Eq. (1), is appropriate only if structural coherence is fully maintained between the Si:As overlayer and the Si substrate, i.e., in the absence of a network of misfit dislocations which relax the in-plane strain by accommodating the difference in equilibrium lattice parameters $a_{\mathrm{Si:As}}$ and a_{Si}. Electron micrographs of the as-laser-annealed Si:As sample showed no misfit dislocations. Interstitial dislocation loops were seen in some areas below the As-containing layer, where laser melting had not penetrated deep enough to remove fully the end-of-range implantation damage. These defects cause local lattice expansion.[13] However, the present x-ray rocking curves are dominated by the lattice strain caused by As incorporation, which is negative for the as-laser-annealed sample.

As suggested by Yokata,[14] we consider that the lattice parameter change caused by doping consists of two components: one local in nature and due to atom size differences, β_{size}, e.g., the cores of dopant atoms or the localized electronic screening of the core at the impurity, and another, $\beta_{e,h}$, due to the hydrostatic deformation potential for the band edge occupied by the free carriers, electrons e or holes h, from the dopants;

$$\beta_{\mathrm{total}} = \beta_{\mathrm{size}} + \beta_{e,h}. \tag{3}$$

We have used the EXAFS result for the As-to-Si distance in Si:As,[4] $d_{\mathrm{AsSi}} = 2.41 \pm 0.02$ Å, together with Vegard's law[15] to estimate the contribution of atom size differences to the actual, experimentally determined lattice parameter for Si:As. Vegard's law is closely followed for isoelectronic covalent alloys, e.g., Si-Ge alloys[16] and for GaAs-InAs alloys.[17] In applying Vegard's law, we have taken the end-point structures to be diamond cubic Si and a hypothetical zinc-blende AsSi. For pure Si, the nearest-neighbor distance is $d_{\mathrm{SiSi}} = 2.35$ Å and $a_{\mathrm{Si}} = (4/3^{1/2}) d_{\mathrm{SiSi}}$. For the nearest-neighbor distance in zinc-blende AsSi, we use the "natural" AsSi bond length[18] $d^{\mathrm{nat}}_{\mathrm{AsSi}}$, so

$$a_{\mathrm{AsSi}} = (4/3^{1/2}) d^{\mathrm{nat}}_{\mathrm{AsSi}}, \tag{4}$$

with

$$d^{\mathrm{nat}}_{\mathrm{AsSi}} = \tfrac{4}{3} (d_{\mathrm{AsSi}} - \tfrac{1}{4} d_{\mathrm{SiSi}})$$

$$= \tfrac{4}{3} d_{\mathrm{AsSi}} - \tfrac{1}{3} d_{\mathrm{SiSi}} = 2.43 \pm 0.02\ \text{Å}. \tag{5}$$

The prediction from Vegard's law for the lattice parameter dependence on N_{As} resulting solely from atom size

differences for Si:As is then given by

$$\beta_{\rm size} = \frac{\Delta a}{a N_{\rm As}} = +(1.4 \pm 0.3)\times 10^{-24}\ {\rm cm}^3. \qquad (6)$$

For $N_{\rm As} = 5\times 10^{21}$ As cm^{-3} this predicts an expansion $\Delta a/a = (7.0\pm 1.5)\times 10^{-3}$ relative to pure silicon.

Using the EXAFS result and Vegard's law for $\beta_{\rm size}$ and the lattice parameter result for $\beta_{\rm total}$, we obtain for Si:As

$$\beta_e = \beta_{\rm total} - \beta_{\rm size} = -(1.8\pm 0.4)\times 10^{-24}\ {\rm cm}^3. \qquad (7)$$

The conduction-band-edge deformation potential a_c corresponding to this value of β_e is[5]

$$a_c = -3B\beta_e = +3.3 \pm 0.7\ {\rm eV}, \qquad (8)$$

where B is the bulk modulus for Si, 0.61×10^{24} eV/cm^3.

Deformation potentials were introduced originally to describe the effect of phonons on mobilities of electrons and holes in semiconductors.[5] It has been suggested that the same type of deformation potential is appropriate for describing the effects of electrons and holes from donors and acceptors on the lattice parameters of semiconductors.[2,5,14] Recent first-principles calculations by Van de Walle and Martin[1] using local-density-functional theory and *ab initio* pseudopotentials yield $a_c = +3.1 \pm 1.0$ eV or $\beta_e = -(1.7\pm 0.5)\times 10^{-24}$ cm^3, which are consistent with the present work.

Calculations of β_e and a_c for Si by Cardona and Christensen[2] with the linear muffin-tin-orbital method have given $\beta_e = -0.3\times 10^{-24}$ cm^3 and $a_c = +0.6$ eV, which are a factor of about 6 smaller than observed experimentally. Nolte, Walukiewicz, and Haller[19] recently reported deformation potentials derived from observed pressure derivatives of acceptor energy levels for Pt and Pd in Si. Their results, $a_c = +2.4$ eV and $\beta_e = -1.3 \times 10^{-24}$ cm^3, have the correct sign but are about 30% smaller than the present experimental result.

Further refinements in comparison of experiments and theory include effects of (100) uniaxial strain lifting degeneracy of conduction-band minima[1] and of degenerate conduction electrons contributing to the hydrostatic deformation potential.[20] However, we do not discuss these effects further, because they are smaller than other uncertainties in experimental and theoretical results noted above.

For Si:As samples annealed at 200, 300, 400, 500, and 600 °C for 30 min, the lattice parameters and the electrical resistivity ρ_a/ρ_0 increase monotonically with annealing temperature, as illustrated by the rocking curves in Fig. 2 and by the resistivity and lattice parameter changes in Fig. 3. Taking the carrier concentration $n_e = N_{\rm As}\rho_0/\rho_a$, these results are consistent with the deformation potential component of the lattice parameter change, $n_e\beta_e$, becoming less important as the dopant atoms become electrically inactive. Reduction of the carrier concentration increases the lattice parameter since $\beta_e < 0$, and reduction of carrier concentration increases the electrical resistivity.

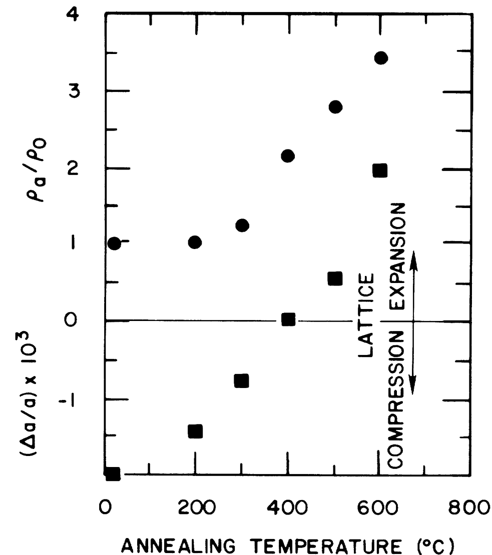

FIG. 3. Normalized resistivities ρ_a/ρ_0 and lattice parameter changes $\Delta a/a$ for Si:As samples annealed for 30 min at different temperatures.

Pandey *et al.*[9] have proposed that As atoms in heavily doped Si become electrically inactive by forming $\rm As_4$-vacancy complexes which are coherent with the Si lattice. In these complexes, the As atoms are displaced from substitutional sites by ~0.17 Å toward the associated vacancy,[6,21] thereby accommodating the As—Si bonds being somewhat longer than the Si—Si bonds with less long-range strain than for isolated, substitutional As in Si. Therefore, $\beta_{\rm size}$ is expected to become smaller with increasing annealing temperature, as more As atoms are incorporated in $\rm As_4$-vacancy complexes and become electrically inactive.

With $\beta_e = -1.8\times 10^{-24}$ cm^3 from Eq. (7), $\Delta a/a$ and ρ_a/ρ_0 from Fig. 3, and

$$\beta_{\rm size} = \frac{\Delta a}{a N_{\rm As}} - \frac{\rho_0\beta_e}{\rho_a}, \qquad (9)$$

from Eq. (3), we have $\beta_{\rm size} = 1.4\times 10^{-24}$ cm^3 for the as-laser-annealed sample but decreasing with increasing annealing temperature to 0.9×10^{-24} cm^3 for 600 °C, in qualitative agreement with the $\rm As_4$-vacancy proposal.[9]

We acknowledge helpful discussions with M. Cardona, S. R. Herd, K. C. Pandey, J. Tersoff, and C. G. Van de Walle.

[a]Also, Department of Materials Science Engineering, MIT, Cambridge, MA 02139. Present address: Department of Electrical and Computer Engineering, University of California at San Diego, La Jolla, CA 92092.

[1]C. G. Van de Walle and R. M. Martin, to be published. See also, C. G. Van de Walle and R. M. Martin, Phys. Rev. B **35**, 8154 (1987).

[2]M. Cardona and N. E. Christensen, Phys. Rev. B **35**, 6182 (1987), and **36**, 2906(E) (1987).

[3]M. Scheffler, Physica (Amsterdam) **146B**, 176 (1987).

[4]A. Erbil, W. Weber, G. S. Cargill, III, and R. F. Boehme, Phys. Rev. B **34**, 1392 (1986).

[5]J. Bardeen and W. Shockley, Phys. Rev. **80**, 72 (1950); R. W. Keyes, IBM J. Res. Dev. **5**, 266 (1961).

[6]A. Erbil, G. S. Cargill, III, and R. F. Boehme, Mater. Res. Soc. Symp. Proc. **41**, 275 (1985).

[7]C. W. White, P. P. Pronko, S. R. Wilson, B. R. Appelton, and R. T. Young, J. Appl. Phys. **50**, 3261 (1979).

[8]D. Nobili, A. Carabelas, G. Celotti, and S. Solmi, J. Electrochem. Soc. **130**, 922 (1983).

[9]K. C. Pandey, A. Erbil, G. S. Cargill, III, R. F. Boehme, and David Vanderbilt, Phys. Rev. Lett. **61**, 1282 (1988).

[10]A. Erbil, G. S. Cargill, III, R. Frahm, and R. F. Boehme, Phys. Rev. B **13**, 2450 (1988).

[11]Lattice compression of this order for Si:As prepared by ion implantation and low-temperature furnace annealing has been reported by M. Nemiroff and V. S. Speriosu, J. Appl. Phys. **58**, 3735 (1985). See also V. S. Speriosu, J. Appl. Phys. **52**, 6094 (1981).

[12]J. Hornstra and W. J. Bartels, J. Cryst. Growth **44**, 513 (1978).

[13]Much higher densities of interstitial dislocation loops occur for solid-phase epitaxial regrowth. For example, see results of electron microscopy and x-ray rocking curves in F. Cembali, M. Servidori, and A. Zani, Solid State Electron. **28**, 933 (1985); see also Ref. 11.

[14]I. Yokota, J. Phys. Soc. Jpn. **19**, 1487 (1964).

[15]L. Vegard, Z. Phys. **5**, 17 (1921); J. D. Eshelby, Solid State Phys. **3**, 79 (1956); J. Friedel, Philos. Mag. **46**, 514 (1955).

[16]See, for example, data cited in Fig. 1 of R. A. Logan, J. M. Rowell, and F. A. Trumbore, Phys. Rev. **136**, A1751 (1954).

[17]J. C. Mikkelsen and J. B. Boyce, Phys. Rev. B **28**, 1730 (1983).

[18]C. K. Shih, W. E. Spicer, W. A. Harrison, and A. Sher, Phys. Rev. B **31**, 1139 (1985); E. A. Kraut and W. A. Harrison, J. Vac. Sci. Technol. B **3**, 1267 (1985).

[19]D. D. Nolte, W. Walukiewicz, and E. E. Haller, Phys. Rev. B **36**, 9392 (1987).

[20]M. Combescot, R. Combescot, and J. Bok, Europhys. Lett. **2**, 31 (1986).

[21]W. K. Chu and B. J. Masters, in *Laser-Solid Interactions and Laser Processing—1978,* edited by S. D. Ferris, H. J. Leamy, and J. M. Poate, AIP Conference Proceedings No. 50 (American Institute of Physics, New York, 1979), p. 305.